

Investigating Diagenetic Alteration as a Cause of Dental Staining in an Historic Tenant Farmer Burial

John V. Dudgeon<sup>1\*</sup>

S. Homes Hogue<sup>2</sup>

Hector Neff<sup>3</sup>

PLEASE DO NOT CIRCULATE OR CITE WITHOUT PERMISSION OF AUTHORS

---

<sup>1</sup>Department of Anthropology and Center for Archaeology, Materials and Applied Spectroscopy (CAMAS), Idaho State University, 921 South 8<sup>th</sup> Avenue, Pocatello, ID 83209, dudgeon@isu.edu.

\*corresponding author

<sup>2</sup>Department of Anthropology, Ball State University, 2000 West University Avenue, Muncie, IN 47306, shogue@bsu.edu.

<sup>3</sup>Department of Anthropology and Institute for Integrated Research in Materials Environments, and Society (IIRMES), California State University Long Beach, 1250 Bellflower Blvd., Long Beach, CA 90840, hneff@csulb.edu.

**Title:** Investigating Diagenetic Alteration as a Cause of Dental Staining in an Historic Tenant Farmer Burial

**Article Type:** Full Length Article

**Keywords:** Laser Ablation ICP-MS; SEM-EDS; Diagenesis; Dental Enamel Staining; Trace Metals

**Manuscript Region of Origin:** USA

**Abstract:** In this paper we report on Laser Ablation Inductively Coupled Plasma Mass Spectrometry (LA-ICP-MS) and Scanning Electron Microscopy – Energy Dispersive X-ray Spectroscopy (SEM-EDS) of black-stained dentition from a late nineteenth century tenant farmer cemetery in Lowndes County, Mississippi. This analysis was conducted for three principal reasons: (1) to confirm the organic or inorganic nature of the black staining on anterior dentition; (2) if inorganic, to determine whether the staining was characteristic of precipitation of soil-derived trace elements or of corroded grave hardware in proximity to the skeleton; and (3) to evaluate LA-ICP-MS as a technique to perform depth profiling of trace element signatures, to investigate the process of diagenesis of mineralized tissues. We show here that LA-ICP-MS, coupled with SEM-EDS is a viable technology to measure the compositional variability in mineralized tissues and offers significant advantages over either technology by itself.

### Highlights

- We combine LA-ICP-MS and SEM-EDS to study micro-scale chemistry at trace element concentrations
- We demonstrate that LA-ICP-MS can perform spatially-discrete trace element analyses in x, y and z planes, yielding true three dimensional analysis
- Our results show that micro-scale trace element chemistry adds novel data to bioarchaeological interpretations of diagenesis and post-depositional alteration
- We frame testable hypotheses for the origin and differential extents of enamel staining

## Introduction

In 2005, professionals and students from Mississippi State University excavated a late 19<sup>th</sup> century African American cemetery in Lowndes County, Mississippi (Hogue and Alvey 2006). The project was necessitated due to the inadvertent discovery of a Historic Period cemetery (Pepper Hill I - 22LO998) during the excavation of a water-line ditch, and seventeen burials were recovered during the salvage operation. One individual, Burial 15, a young female around 18 years old at the time of death, exhibited pronounced black staining on the buccal anterior maxillary teeth (**Figure 1**). Based on this initial discovery, we were interested in determining whether the visible staining was associated with a cultural behavior such as smoking or chewing tobacco, was produced through diet or some systemic cause, or occurred posthumously.

Few available publications investigate dental staining in archaeological collections. In modern dentistry, discolorations of the teeth are known to result from both intrinsic and extrinsic factors. Intrinsic tooth staining occurs when discoloration occurs during tooth development usually due to some form of metabolic stress (Watts and Addy 2001). Several physiological conditions such as congenital heart disease, neonatal hepatitis, and bile duct defects can create dental discoloration which varies from yellow to brown (Ortner 2003; Watts and Addy 2001). Systemic drug use can also discolor the dentition. For example, tetracycline can create tooth discoloration during fetal development with color changes ranging from yellow to brown depending on the dosage (Watts and Addy 2001). Extrinsic tooth discoloration is caused by abnormal environmental conditions. Brown to dark brown discoloration on the enamel surface is linked to excessive fluoride in the diet, tobacco use, and chewing betel nut (Ortner 2003). Dissolved iron and manganese in drinking water causes reddish-brown or black stains on clothing and could potentially affect tooth color (Herman 1996). Schuurs et al. (1987) identified the loss of enamel and a deep black stain on the teeth of a 40 year old diabetes patient as possibly caused by consuming cheap wine or chewing cayenne on a daily basis. Occupational and drug exposure to metallic salts can increase extrinsic staining. It is well-documented that black stained teeth are associated with individuals who use iron supplements or work in iron manufacturing (Watts and Addy 2001). Etiological explanations for the observed staining were initially considered, but the presence of staining on the occlusal tooth surfaces made these unlikely (see Ortner 2003:605).

Post-depositional contamination has also been recognized as causing tooth discoloration. Manganese oxide soil deposited posthumously was the probable cause of black enamel tooth stains on a

medieval skeletal collection from Norway (Stermer et al. 1996). Like the Burial 15 specimen, the blackish stain observed on these teeth could not be removed (Stermer et al. 1996), and appeared to have penetrated into the surface of the enamel under light microscopy. The differential staining between the mandibular and maxillary teeth could be related to post-mortem alteration under conditions of dental malocclusion (*retrognathia*); however, during the decomposition process the mandible had dropped away from the cranium while the maxilla had collapsed within the cranial vault.

Post depositional diagenetic alteration was initially considered but discounted, on account of the lack of similar enamel staining in other individuals. The unusual color and patterning of the staining made macroscopic identification difficult and samples of the affected dentition were submitted for compositional analysis using laser ablation inductively coupled plasma mass spectrometry (LA-ICP-MS) and scanning electron microscopy energy dispersive x-ray spectroscopy (SEM-EDS) in an effort to determine whether the staining was comprised of organic or inorganic constituents.

### **Dental Staining**

For this study, we hypothesized that the occurrence of blackish staining on the teeth was the result of inorganic oxide deposition (possibly manganese or iron) on or near the enamel surface. We address the alternate hypotheses that the source of the staining is either, 1) native soil elements dissolved in pore water; or 2) corroded metal coffin hardware. Lastly, we attempt to determine the extent of the staining on the tooth, from surface—inward, to understand the processes favoring the formation of these types of stains on certain individuals.

### **Materials**

Fourteen maxillary and thirteen mandibular teeth from Burial 15 showed black staining in some areas of the enamel. Solid discoloration measured 10yr 2/1 [black] using the Munsell color chart while more mottled discoloration was 10YR 4/1 [dark gray] (Munsell 2000). The maxillary incisors had the most staining (**Figure 1**), occurring over most of the buccal enamel surface and percentage of the actual enamel area stained decreased in frequency towards the molars. In comparison, the mandibular teeth showed little staining. For the elemental analysis, the left central incisor was used because a fracture created a clean anterior-posterior break in the tooth, exposing the interior surface of the dentinal crown. Using the internal tooth surface, we attempted to determine whether the stain was superficial on the enamel surface or associated with physiological or dietary causes during individual development.

For comparative purposes a central incisor from Burial 4, an adult male, was also assayed. This incisor showed no visible staining on the enamel surface.

## **Methods**

A combined analytical methodology employing LA-ICP-MS (New Wave UP 213 nm Laser Ablation System and Thermo X-series II ICP-MS with GCMS dual-inlet interface) for trace elements (defined here as  $< 1000 \mu\text{g/g}$ , or ppm) and SEM-EDS (FEI Quanta 200F SEM with a Bruker Quantax 200 EDS) for major elements (detected at greater than 0.15 %/wt., or  $1500 \mu\text{g/g}$ , or ppm) was used to provide internal standard calibration for LA-ICP-MS intensity signals and to assess the overall level of preservation of the samples. Multi-element compositional data was collected by LA-ICP-MS, and subsequent calibration data for major element internal standardization was collected proximal to each ablation site using SEM-EDS. An internal standardization correction was applied to the raw LA-ICP-MS concentration data to generate the final, normalized concentration of minor and trace elements.

### *Analytical standards and experimental standardization methods*

A combination of synthetic hydroxyapatite (HA) standards and USGS glass standards (GSC-1G, GSD-1G, GSE-1G, BHVO-2G, BCR-2G, BIR-1G) were used to calibrate the ICP-MS signal intensities of the unknown samples. In a paper from the National Institute of Standards and Technology (Chow and Takagi 2001), the authors reported that during research in the chemical properties of calcium phosphates, a novel material was synthesized in the lab that bore close resemblance to bone hydroxyapatite (HA). When mixed with water or a slightly alkaline phosphate buffer, the material would self harden in prismatic crystal lattices that approximated the structure and mineral properties of biological hydroxyapatite. Infusing this powdered mixture with trace elements at known concentration prior to crystallization produces a significantly homogeneous minor and trace element distribution in a hydroxyapatite matrix that is the inorganic stoichiometric equivalent of bone and tooth (i.e., 39% Ca, 18% P, 43% O).

Six standards were prepared to span the range of expected elemental composition in the unknown dental enamel samples (Curzon and Cutress 1983). The first standard was made as an apatite blank, to correct for the possible influence of large concentrations of calcium and phosphorus on other masses ranges that might produce spurious peak data on adjacent masses immediately surrounding the large HA element peaks. Additionally, matrix-matched blank standards allow the detection of impurities in the analytical grade reagents, which could contribute to the observed background in the standard

blank. See Dudgeon (2008) for a description of the procedure for constructing hydroxyapatite laser ablation standards.

In addition to calibrating the unknowns using USGS glass/HA standards, two additional internal standard-type calibrations were performed during and after analysis. The first was an instrumental drift/matrix suppression calibration: Our ICP-MS uses a GCMS-based dual-inlet interface, permitting simultaneous introduction of laser ablation sweep gas plus argon makeup gas, and liquid internal standard. For this analysis, 20 ppb of ruthenium standard in 2.0% trace metal grade HNO<sub>3</sub> was continuously aspirated through a concentric nebulizer upstream of the dual-inlet interface to visualize and correct for instrument drift and matrix suppression, performed on-the-fly by the ICP-MS software. The second calibration used actual major element concentration (normalized weight percent) data measured via SEM-EDS at or proximate to the ablation site to normalize the LA-ICP-MS concentration data to correct for matrix suppression, topographic effects and variation in laser-sample energy coupling. We used the SEM-EDS normalized weight percent of calcium measured at or near the ablation site in the tooth samples to apply a sample-specific correction factor to the LA-ICP-MS concentration data to adjust the LA-ICP-MS calcium values to the measured SEM-EDS values.

While the stoichiometric concentration of calcium in bone hydroxyapatite [Ca<sub>10</sub>(PO<sub>4</sub>)<sub>6</sub>(OH)<sub>2</sub>] is around 39% wt./wt., in living systems calcium concentration by weight varies from this theoretical value due to the carbon/nitrogen organic collagen matrix, and magnesium or sodium substitution at calcium positions in the hydroxyapatite crystal (Gage et al. 1989; Nanci 2008). Because calcium is used to standardize the laser ablation signal intensities for each element acquisition, deviations from the expected stoichiometric concentration affect the accuracy of the concentration determination and should be normalized to replicate SEM-EDS major element data. A minimum of ten replicate SEM-EDS measures of calcium were averaged and the mean value used in the internal standard correction for the tooth raw concentration laser ablation data.

### *Sampling procedures*

Laser ablation was performed using a New Wave UP 213 nm laser ablation system coupled to a Thermo X-series II ICP-MS. The method used was similar to that described in Cucina et al (2007), using sets of bracketing standards around sets of discrete ablation events. Laser ablation ICP-MS has been shown to be an effective method to describe discrete chemical variation in solid biomaterials (Abdullah et al. 2011, Cucina et al. 2006, Cucina et al. 2011, Dudgeon 2008, Nishimoto et al. 2010, Seltzer and

Berry 2005). In this case, the laser permits the controlled ablation of biological layers of enamel, allowing us to determine the source and direction of diffusion of trace elements through the enamel.

The first assays were done on the buccal surface of both specimens where three readings were used to provide an average of typical enamel major, minor and trace element values on the unstained portion of each tooth. Following this procedure, a grid of one hundred fifty 100  $\mu\text{m}$  diameter ablation spots placed at 250  $\mu\text{m}$  intervals were positioned on the internal incisor surface of the black stained tooth to determine the depth of the discoloration on the buccal-lingual aspect. Each laser spot was pre-ablated to remove any immediate surface contamination adhering to the fractured surface from handling or loose sediment and to provide a uniform surface for quantitative laser ablation.

Immediately post-LA-ICP-MS, we imaged and performed energy-dispersive x-ray microanalysis on the ablated sections using the Bruker Quantax 200 EDS on the FEI Quanta 200F SEM, to visualize and map the distribution of major and minor elements on the internal surface of the tooth. The SEM is useful for documenting micro-morphological or histological changes to the structure of the enamel and dentin, such as decalcification, cracking or enamel spalling that might help explain the diagenetic changes in the tooth after burial. See **Table 1** for a summary of instrumental operating parameters.

## Results

When the black stained (Burial 15) and control (Burial 4) teeth were compared, iron emerged as the major addition on and within the black stained tooth, being over 7,200 ppm higher in the black tooth than in the white tooth. Additionally, other transition metals and water-soluble trace metals were enriched in the enamel of the black tooth—consistent with an explanation of metals leaching from the surrounding sediments into the enamel matrix on this sample (**Table 2**). Surface contour maps (**Figure 2**) of element distribution on the fractured surface also indicated the presence of high levels of barium, iron, and manganese on the buccal and occlusal surfaces of the tooth enamel that correspond spatially to the black staining on the tooth enamel. The depth of the staining inward was measured to be less than 500  $\mu\text{m}$  from the buccal enamel surface, suggesting that environmental factors after deposition caused the staining, rather than continued physiological or systemic events during the individual's development.

Imaging the blackish staining under light microscopy shows definitively the dendritic, secondary character of the staining (**Figure 3**). This image was obtained by setting a focal point within the enamel structure, suggesting the precipitation of elements contributing to the staining formed between layers

of enamel. We attempted to discern the actual position of the staining feature by conducting a depth-profiling experiment using LA-ICP-MS to successively ablate precise quantities of enamel and intercalated iron in the HA matrix (**Figure 4**). By varying the laser output power and speed of traverse across the sample, it is possible to effectively sample repeatable quantities of enamel and incorporated trace elements in each pass. Using the SEM to measure the crater depth over a series of laser ablation passes yielded an average ablation depth of approximately 12  $\mu\text{m}$  per pass. **Figure 5** demonstrates the signal generated by iron during each pass of the tooth area shown in **Figure 4**. Based on this data, we conclude the iron staining occupies a region of enamel from the tooth surface to approximately 108 – 120  $\mu\text{m}$  deep, with the majority of the staining occupying the region from 36 – 60  $\mu\text{m}$  from the surface.

In order to test the possibility that water leaching of native trace elements in the sediments were responsible for the observed stains on Burial 15, sediment samples proximate to (but not in) the immediate grave shaft were leached with DI  $\text{H}_2\text{O}$  over a period of several weeks and analyzed using liquid aspiration ICP-MS. Metal concentrations recovered from the water leaching were compared to the LA-ICP-MS results from Burials 15 and 4 (**Figure 6**). The enrichment of the enamel with soluble metals strengthens the hypothesis that soil porewater and/or direct sediment contact was the primary means of transport of these elements (Snyder-Conn et al., 1997). The results show that the increased concentrations of iron, barium, nickel, arsenic and cobalt were most likely caused by posthumous contamination. Rather than passing through the enamel matrix as an ionic solution, precipitation of iron and other trace elements occurred along enamel cracks and fissures, proceeding along the walls of cracks and spreading laterally between enamel layers.

SEM examination of the micro-structural characteristics of the bisecting fracture of the Burial 15 crown showed that the break across the proximal crown probably occurred sometime after the chemical precipitation of water soluble metal elements into the exterior and subsurface enamel, likely from environmental changes after disinterment. Other than some lamellar spalling of enamel from the area immediately surrounding the broken surface, the structural integrity and mineralization of the enamel and underlying dentin was intact, suggesting that the overall health or porosity of the dentition was not the primary cause of the surface staining.

## **Conclusion**

Given the evidence of moderate surficial enrichment of several trace elements proportional to their occurrence in the surrounding sediment, the occurrence of staining on the buccal (versus lingual)

aspect of the anterior teeth of Burial 15 supports the explanation that grave soil or other hardware contact on the outer surface of the teeth produced the blackish staining post mortem. After the decomposition of the soft tissues and the wooden box of the coffin, overlying sediment filled the coffin space and came to rest on the buccal surface of the anterior dentition. Decomposed coffin hardware such as nails and hinges made of iron may have had contact with certain skeletal elements during interment, but our evidence does not suggest that this was the primary agent contributing to the staining. Manganese was often added during the production of plate or cast irons to produce hardening and as an aid in removing impurities such as oxygen and sulfur (Wysor, 1921), and has been implicated as a primary oxide producing dental staining in other archaeological studies (Stermer et al. 1996). However, as there were no differences found in the manganese concentration between Burial 15 (black tooth) and Burial 4 (control), it is unlikely that manganese is implicated as a major constituent of precipitate staining.

The observation of enrichment, relative to sediment concentration in the first row transition metals (e.g., titanium, vanadium, chromium, manganese, iron, cobalt, nickel and copper), and rare earth elements has been modeled for rock varnish systems by Thiagarajan and Lee (2004), who proposed that these elements are physically leached from clay particles in aqueous atmospheric environments, precipitating on underlying solid surfaces. Due to the visual similarity and chemical composition of our dendritic iron precipitation to rock varnish, we suggest that a similar process, albeit in situ, is occurring within the overlying clayey soils in the Pepper Hill I cemetery. The observation of enrichment of elements which are characteristic impurities or historically-important additives to iron—implying human-made iron enrichment—is found to be a trivial similarity, given the evidence for enrichment of particle reactive REEs as described by Thiagarajan and Lee (2004).

In summary, our research suggests the curious blackish coloration discovered on the teeth of burial remains from Pepper Hill I is consistent with post-depositional mineral-based staining on the surface and subsurface enamel, originating in the regional clays found throughout Lowndes County, Mississippi. The limited extent of staining on the anterior dentition of one of approximately seventeen burials is best explained by the combination of interment position, interment depth, grave sediment association and post-mortem deterioration of the outer enamel matrix. Further research is underway to identify the cause of the enamel deterioration on Burial 15, from which we plan to construct a more general model framework for understanding post-depositional trace metal uptake and its effects on mineralized tissues.

## References

- Abdullah, M.M., Ly, A.R., Goldberg, W.A., Clarke-Stewart, K.A., Dudgeon, J.V., Mull, C.G., Chan, T.J., Kent, E.E., Mason, A.Z., Ericson, J.E., 2011. Heavy Metal in Children's Tooth Enamel: Related to Autism and Disruptive Behaviors? *Journal of Autism and Developmental Disorders*, DOI: 10.1007/s10803-011-1318-6.
- Chow, L.C., Takagi, S., 2001. A natural bone cement: A laboratory novelty led to the development of revolutionary new biomaterials, *Journal of Research of the National Institute of Standards and Technology* 106, 1029-1033.
- Cucina, A., Dudgeon, J.V., Neff, H., 2007. Methodological Strategy for the Analysis of Human Dental Enamel by LA-ICP-MS, *Journal of Archaeological Science* 34, 1884-1888.
- Cucina, A., Tiesler, V., Sosa, T.S., Neff, H., 2011. Trace-element evidence for foreigners at a Maya port in Northern Yucatan, *Journal of Archaeological Science* 38, 1878-1885.
- Curzon, M.E.J., Cutress, T.W. (eds.), 1983. *Trace elements and dental disease*, John Wright/PSG Inc., Littleton, Massachusetts.
- Dudgeon, J.V., 2008. *The Genetic Architecture of the Late Prehistoric and Proto Historic Rapa Nui (Easter Islanders)*, Ph.D. Dissertation, University of Hawai'i, Mānoa.
- Gage, J. P., Francis, M. J. O., Triffit, J. T., 1989. *Collagen and Dental Matrices*, Wright, London.
- Hogue, S.H., Alvey, J.S., 2006. Final Report on Archaeological Burial Recovery at Pepper Hill I Cemetery, 22LO998, Lowndes County, Mississippi, *Cobb Institute Archaeological Research Reports* 144 pages.
- Munsell Soil Color Chart, 2000*. Munsell Color Corporation.
- Nanci, A., 2008. *Ten Cate's Oral Histology: Development, Structure, and Function*, 7th edition, Mosby, St. Louis.
- Neff, H., Dudgeon, J. V., 2006. *LA-ICP-MS Analysis of Ceramics and Ceramic Raw Materials from the Gila River Indian Community, Arizona*, Research Report: Institute for Integrated Research in Materials, Environments, and Society, California State University, Long Beach.
- Nishimoto, M.M., Washburn, L., Warner, R.R., Love, M.S., Paradis, G.L., 2010. Otolith elemental signatures reflect residency in coastal water masses, *Environ Biol Fish* 89, 341-356.
- Herman, G.M., 1996. *Iron and Manganese in Household Water*. Prepared for the Extension Housing Specialist Published by: North Carolina Cooperative Extension Service Publication Number: HE-394 Last Electronic Revision: March 1996 (JWM)
- Ortner, D.J., 2003. *Identification of Pathological Conditions in Human Skeletal Remains*. 2nd ed. Smithsonian Institution Press, Washington, D.C.

Schuurs, A.H., Abraham-Inpijn, L., van Straalen, J.P., Sastrowijoto, S.H., 1987. An Unusual Case of Black Teeth, *Oral Surgery, Oral Medicine, Oral Pathology* 64, 427-31.

Seltzer, M., Berry, K., 2005. Laser ablation ICP-MS profiling and semiquantitative determination of trace element concentrations in desert tortoise shells: documenting the uptake of elemental toxicants, *Science of the Total Environment* 339, 253-265.

Snyder-Conn, E., Garbarino, J.R., Hoffman, G.L., Oelkers, A., 1997. Soluble Trace Elements and Total Mercury in Arctic Alaskan Snow, *Arctic* 50, 201–215.

Stermer, E.M., Rises, S., Fisher, P.M., 1996. Trace Element Analysis of Blackish Staining on the Crowns of Human Archaeological Teeth, *European Journal of Oral Science* 104, 253-261.

Thiagarajan, N., Lee, C., 2004. Trace element evidence for the origin of desert varnish by direct aqueous atmospheric deposition, *Earth and Planetary Science Letters* 224, 131-141.

Watts, A., Addy, M., 2001. Tooth Discoloration and Staining: A Review of the Literature, *British Dental Journal* 190, 309-316.

Wysor, H., 1921. *Metallurgy: A Condensed Treatise for the Use of College Students and Any Desiring a General Knowledge of the Subject*, The Chemical Publishing Company, Eaton, Pennsylvania.

**Table 1.** Instrumental parameters for LA-ICP-MS analysis.

---

Laser Ablation Device	New Wave UP213 Nd:YAG
Wavelength	213 nm
Energy	0.6 mJ
Spot size	100 $\mu\text{m}$ (imaged aperture)
Fluence	7.35 $\text{J cm}^{-2}$
Rep rate	20 Hz
Passes	Single, spot mode
Depth/pass	5 $\mu\text{m}$
Laser Output	60%
Laser on time	40 seconds, spot mode
Sweep gas (He)	0.313 $\text{L min}^{-1}$ , constant
ICP-MS	Thermo X-series II
Detector	Discrete Dynode Electron Multiplier
RF power	1403.92 W
Nebulizer flow rate (Ar, dual inlet system)	0.710 $\text{L min}^{-1}$
Sample gas flow rate (He)	0.313 $\text{L min}^{-1}$
Dual-inlet aspirated solution (Int. Std.)	Ruthenium, 20 ppb in 2.0% $\text{HNO}_3$
Scan mode	Peak Jumping
Number of Sweeps	35
Dwell Time at Standard Resolution	10 ms
Dwell Time at High Resolution	2 ms (Na, Si, P)
Channels Per Mass	1
Channel Spacing	0.02

---

**Table 2.** Comparison of LA-ICP-MS concentration data for tooth samples and liquid aspiration of DI H<sub>2</sub>O-leached sediment proximate to the graves site. All concentration data in µg/g (ppm). Underlined values indicate disparity in Black Tooth – Control Tooth values greater than 2x. Bold values indicate disparity greater than 5x.

Element	Burial 15 Black Tooth	Burial 4 Control Tooth	Associated Sediment
Mg	476.74	475.05	40.11
Ti	21.29	12.10	5.93
V	<u>1.21</u>	0.58	1.49
Cr	0.23	0.24	1.17
Mn	559.14	645.51	13.72
Fe	<b><u>8379.33</u></b>	1144.69	446.20
Ni	<u>7.26</u>	2.13	0.27
Co	<b><u>23.22</u></b>	0.57	0.16
Zn	174.13	<u>336.82</u>	0.83
As	<b><u>12.13</u></b>	1.14	0.33
Sr	<u>291.98</u>	125.13	4.12
Y	13.34	<b><u>143.01</u></b>	0.15
Ba	<b><u>46.39</u></b>	8.36	1.91
La	35.26	<b><u>185.17</u></b>	0.30
Ce	131.06	<u>381.10</u>	0.88
Pr	4.97	<b><u>24.03</u></b>	0.08
Nd	22.48	<b><u>126.44</u></b>	0.31
Pb	19.73	<b><u>112.70</u></b>	0.20
U	<u>1.84</u>	0.91	0.04

## List of Figures

**Figure 1.** Central maxillary incisors, Burial 15, Pepper Hill I cemetery.

**Figure 2.** Surface contour maps of element distributions from spot analysis on broken surface of maxillary incisor, Burial 15. Maps of concentration ( $\mu\text{g/g}$ , ppm) for elements iron, barium and manganese.

**Figure 3.** Light microscope image of dark staining, buccal surface maxillary incisor, Burial 15. Note fern-like, dendritic pattern of dark staining on enamel interior along surface crack.

**Figure 4.** LA-ICP-MS transient signal analysis (bottom) across irregularly stained surface (top), buccal anterior incisor. Yellow line (top) indicates the area ablated by laser. Long tail on left of transient signal (bottom) is the sample blank (i.e., laser off, ICP-MS background).

**Figure 5.** Iron signal data, buccal incisor surface, Burial 15. Signal data in intensity counts per second (ICPS), y-axis. Time series measured left to right, x-axis. Laser ablation passes (enamel surface inward) front to rear, z-axis.

**Figure 6.** Tooth concentration data compared to sediment concentration data for Burial 15 (Black Tooth) and Burial 4 (Control Tooth). Sediment concentration derived using liquid aspiration ICP-MS; Tooth concentration derived using LA-ICP-MS. All values plotted as  $\log_{10}$  ppm of concentration.



**Figure 1.** Central maxillary incisors, Burial 15, Pepper Hill I cemetery. Lowndes County, Mississippi.

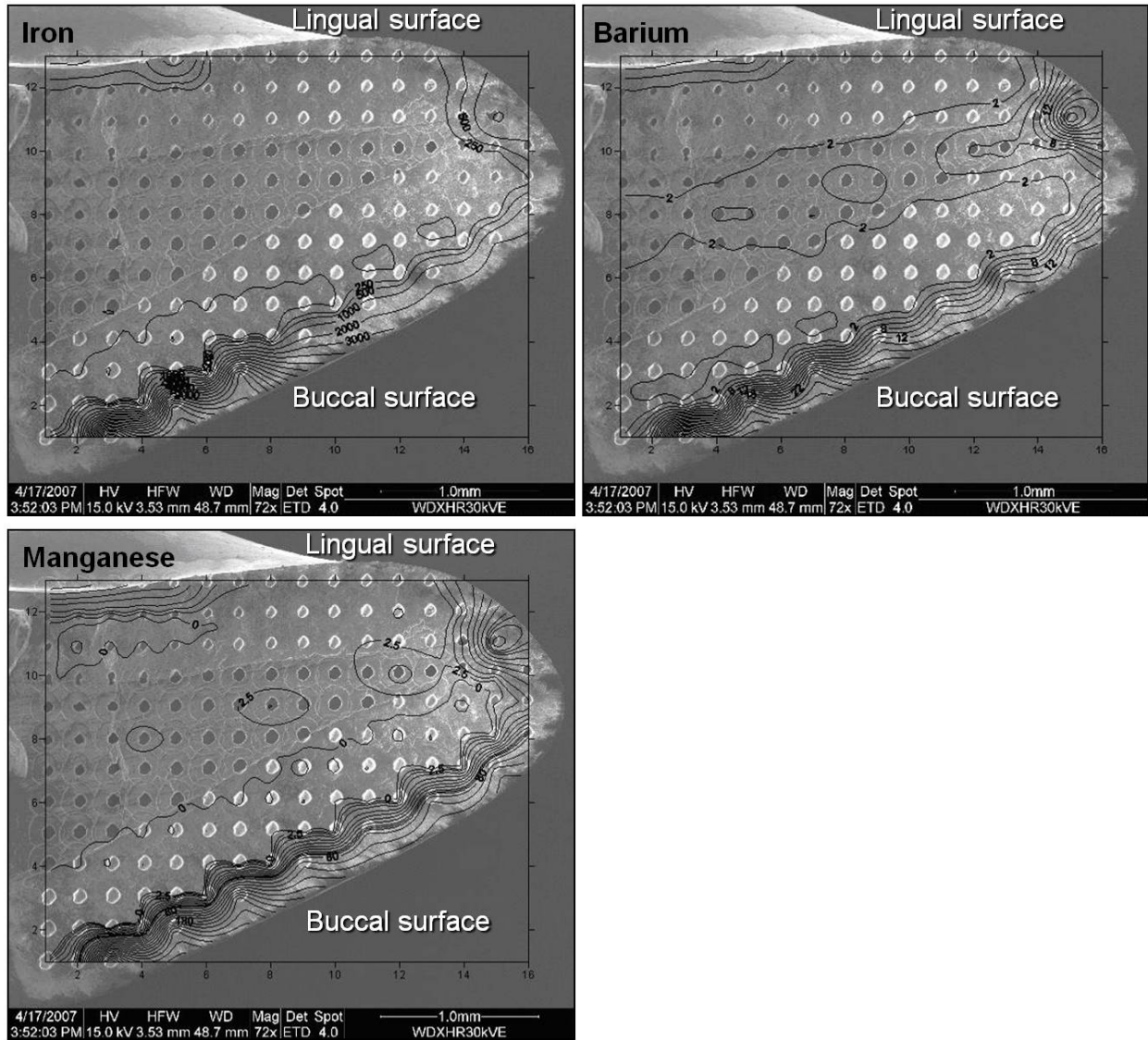


**Figure 2.** Surface contour maps of element distributions from spot analysis on broken surface of maxillary incisor, Burial 15. Maps of concentration ( $\mu\text{g/g}$ , ppm) for elements iron, barium and manganese.

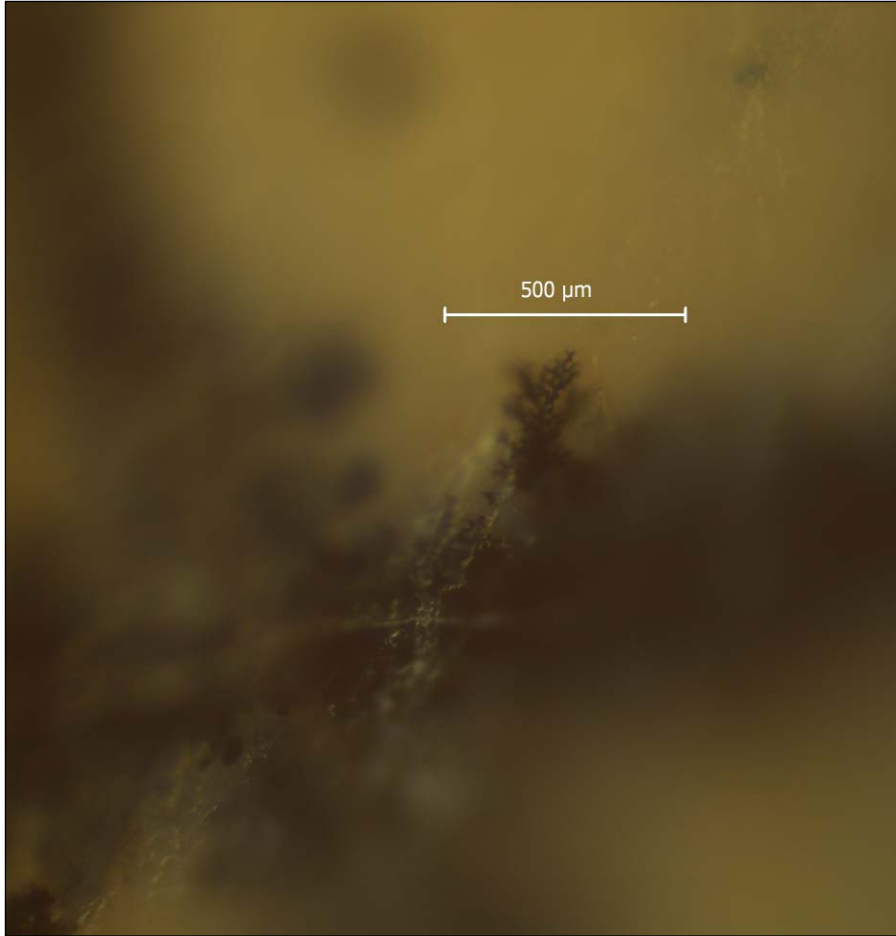


**Figure 3.** Light microscope image of dark staining, buccal surface maxillary incisor, Burial 15. Note fern-like, dendritic pattern of dark staining on enamel interior along surface crack.

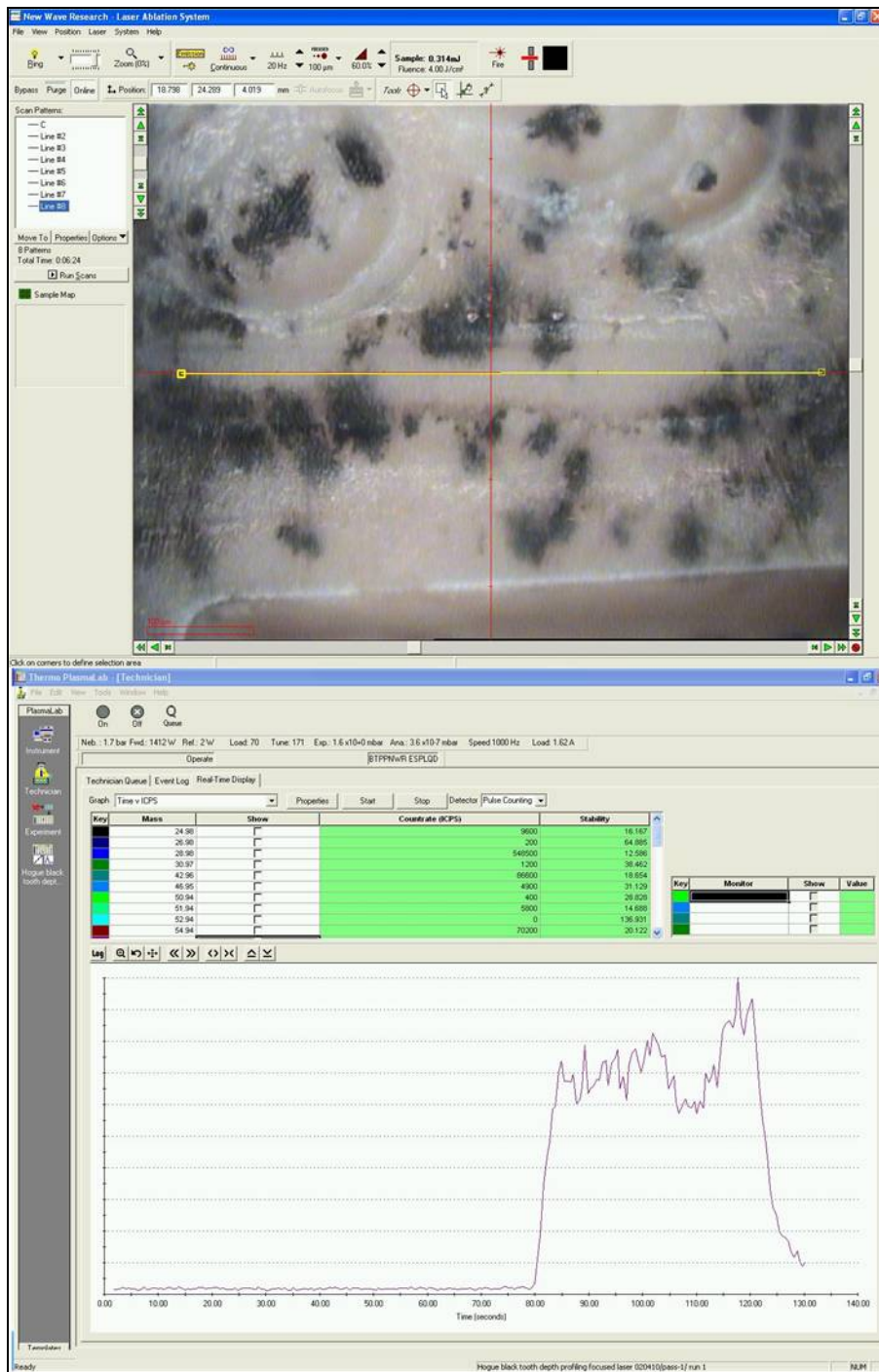


**Figure 4.** LA-ICP-MS transient signal analysis (bottom) across irregularly stained surface (top), buccal anterior incisor. Yellow line (top) indicates the area ablated by laser. Long tail on left of transient signal (bottom) is the sample blank (i.e., laser off, ICP-MS background).

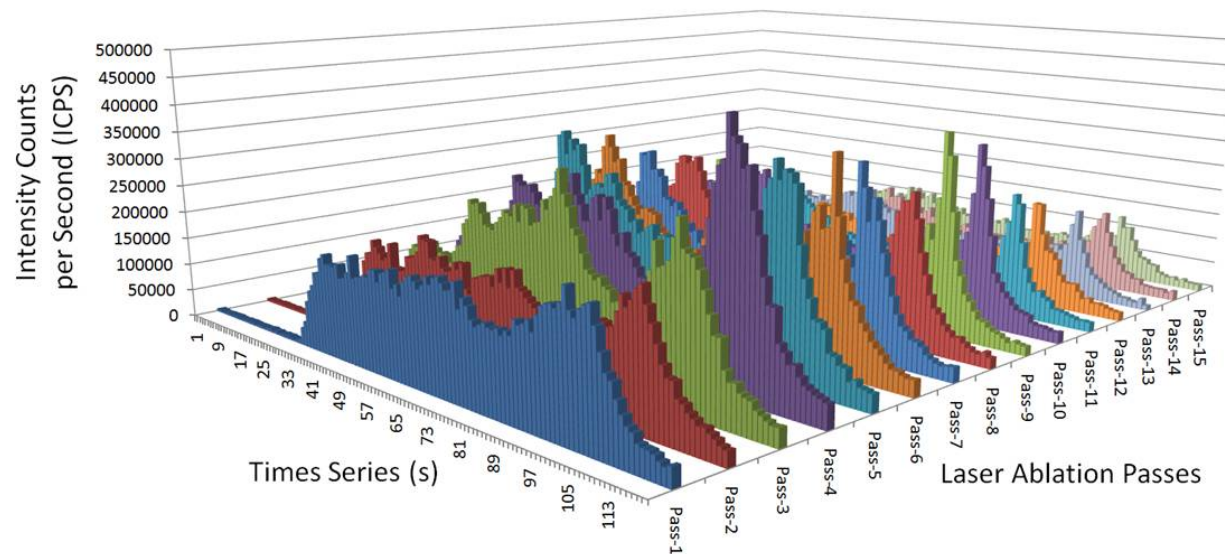


**Figure 5.** Iron LA-ICP-MS intensity data, buccal incisor surface, Burial 15. Signal data in intensity counts per second (ICPS), y-axis. Time series measured left to right, x-axis. Laser ablation passes (enamel surface inward) front to rear, z-axis. Average depth per pass is  $\sim 12 \mu\text{m}$ .

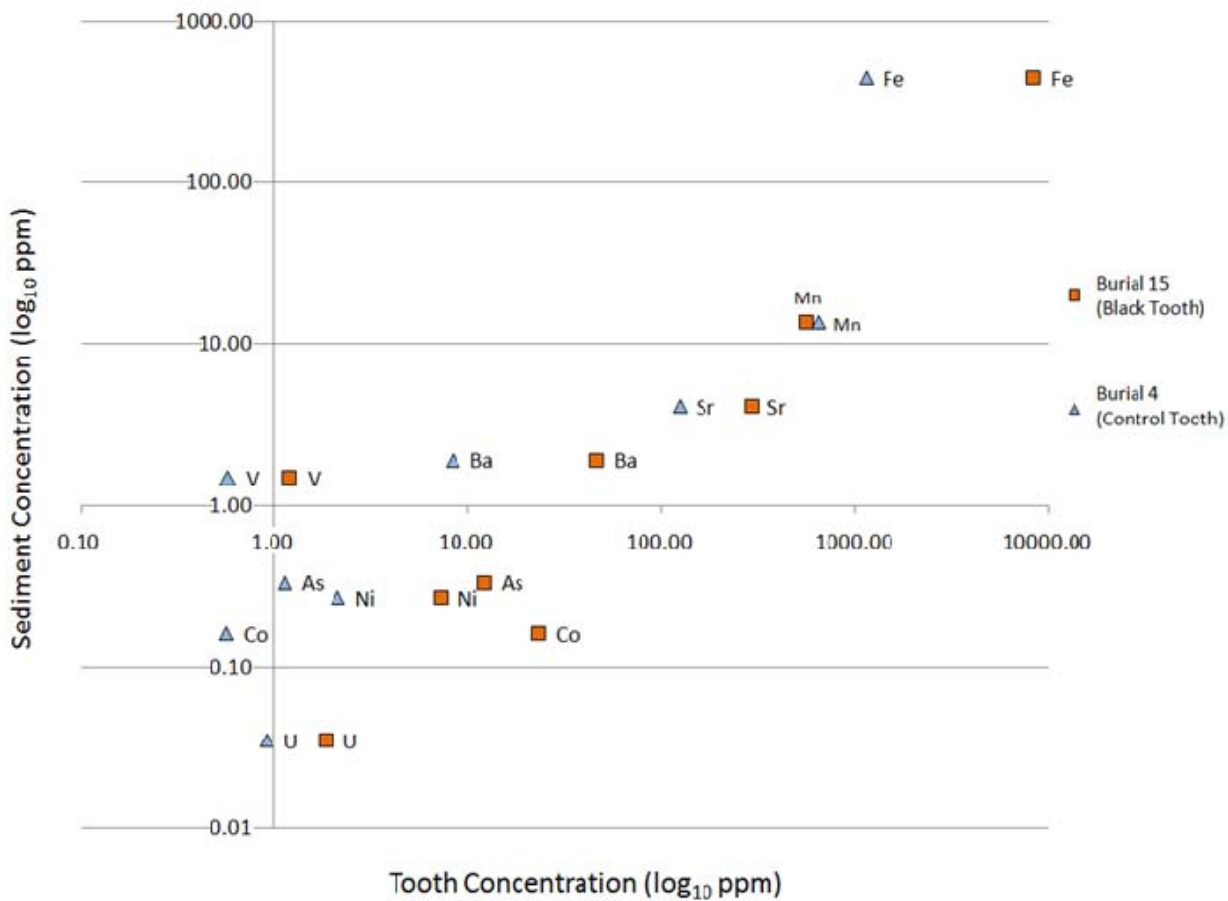


**Figure 6.** Tooth concentration data compared to sediment concentration data for Burial 15 (Black Tooth) and Burial 4 (Control Tooth). Sediment concentration derived using liquid aspiration ICP-MS; Tooth concentration derived using LA-ICP-MS. All values plotted as log<sub>10</sub> ppm of concentration.